OPEN ACCESS

University of BRISTOL

Tan, C. M., Chin, C. M., Sim, M. L., & Beach, M. A. (2007). Indoor MIMO channel modelling with modified Gumbel's bivariate exponential expression based on double-directional correlation properties. In IEEE International Conference on Communications, 2007 (ICC '07), Glasgow. (pp. 2516 - 2521). Institute of Electrical and Electronics Engineers (IEEE). 10.1109/ICC.2007.416

University of Bristol - Explore Bristol Research

General rights

Indoor MIMO Channel Modelling with Modified Gumbel's Bivariate Exponential Expression Based on Double-Directional Correlation Properties

C. M. Tan[1], C. M. Chin[1], M. L. Sim[1], and M. A. Beach[2]

[1]British Telecom Asian Research Centre,
Group Chief Technology Office.
Emails: {chormin.tan; eric.chin; mohlim.sim}@bt.com

[2]Centre for Communications Research,
University of Bristol, UK.
Email: m.a.beach@bristol.ac.uk

Abstract- **Precise measurement and modelling of the Direction of Arrival (DoA) and Direction of Departure (DoD) in the Multiple-Input Multiple-Output (MIMO) channel based on their correlation properties and joint distributions have not been investigated properly. Our main contribution in this paper is two fold. Firstly, based on a *modified Gumbel's bivariate exponential* approach, we propose a generic indoor MIMO channel modelling framework particularly for the double-directional '*general trend*' that has been observed in these dual-spatial domains. Secondly, we propose a transformation technique to generate the pair wise DoA and DoD components incorporating the correlation properties of the variates around the full azimuth range. Results show that the newly proposed modelling approaches provide a good match to the real data, offering an alternative hassle-free method to generate realistic directional-based stochastic MIMO channel responses in different indoor environments.**

I. INTRODUCTION

Owing to the advantages of MIMO communications, many wireless systems have started to incorporate MIMO technologies into their standards, e.g. IEEE 802.11n, IEEE 802.16, and the enhanced technical specifications in 3GPP and 3GPP/2. Following that, realistic MIMO channel models are required in order to assess the performance of these improved systems, and this requires accurate DoA and DoD information of the multipath components (MPCs), and the ability to isolate responses of antennas from the measured channels through offline processing. In short, these models must be able to reproduce accurate correlation properties of the radio propagation mechanisms as viewed from both transmitter (Tx) and receiver (Rx), where excellent discussions and reviews of different modelling approaches can be found in European COST 273 [1], IST WINNER [2], and NEWCOM [3] projects.

The IEEE 802.11 TGn channel models [4] in general employ the 'Kronecker' approach when generating the MIMO channel responses, where the individual transmit or receive correlation matrix is constructed separately based on the characterised directional distributions of the MPCs, with no consideration of the correlations of DoAs and DoDs. Similar assumption is also made in the IST METRA 'Kronecker' based MIMO channel model [5]. However, it has been shown that 'Kronecker' model that fails to render the realistic propagation mechanism of MPCs would cause systematic capacity mismatch in a MIMO channel [6], which is often the case when the spatial correlation

of Tx and Rx (or in this case DoA and DoD) is assumed independent. The authors in [7] proposed some closed-form solutions to construct the element (spatial) correlation matrix of an array based on MPC's single-directional information, but did not address methods of simultaneous matrix construction at both ends using double-directional knowledge. Further, although the COST 273 [1] and IST WINNER [2] MIMO models are by far two of the most comprehensive models that have been developed, they do not consider the joint probability density and correlations of DoAs and DoDs explicitly.

In summary, most, if not all, MIMO channel models do not address the correlation properties of DoAs and DoDs explicitly through real observation of measurement results, which in effect points to the main reason of mismatch between the simulated and measured MIMO channel responses. This is especially so when considering their joint distributions around the entire azimuth plane (i.e. 360°) at both ends of the communication links. Further, the non-negligible correlation coefficients of DoA and DoD in some environments imply that the joint statistics of both parameters in these environments are nonseparable, and must be described properly by their joint distribution functions as applied to different radio environments.

Here, the paper aims to describe a new modelling approach for the joint distributions of DoA and DoD components, as well as their joint power density. Primarily, the model considers the '*general trend*' (details described later) observed in these domains, which is similar in many picocell environments that have been investigated [8][9]. In terms of double-directional propagation modelling, we propose a '2-D Laplacian-like', or *modified Gumbel's bivariate exponential* joint distribution to model the MPCs and power density in the dual-spatial domains, where a good match to the real data can be achieved. In addition, a hassle-free transformation technique is also proposed to generate the pair wise DoA and DoD variates with certain correlation coefficient.

It should be noted that the paper emphasises on the indoor MIMO channel modelling framework specifically for the double-directional '*general trend*' of MPCs, which could form part of the modelling steps of a MIMO propagation channel, but not the complete modelling procedure. Hence, the proposed modelling approaches can also act as an overlay implementation of other directional-based models, which could effectively further increase the overall accuracy and reliability of the models.

II. MIMO Measurements and Summary of Results

A. Indoor Measurement Campaigns

Several extensive dynamic wideband double-directional/ MIMO measurement campaigns were conducted in four different indoor environments typical for wireless network deployments: office, corridor, open foyer, and laboratory. The environments were highly cluttered, with standard indoor furniture throughout. There was no restriction imposed on the environments, as people were allowed to move around freely (to emulate real wireless scenarios). Different propagation conditions were considered: populated, unpopulated, line of sight (LOS), obstructed or non-LOS (OLOS/NLOS), etc.

The measurements employed advanced techniques capable of providing high-resolution support. A novel feature of the measurement setup was the ability to provide instantaneous full azimuth views at both ends by employing a pair of 16-element uniform circular patch arrays. The sounding bandwidth was set to 120 MHz (centred at 5.2 GHz), and the period of the transmitted multitone signal was 0.8 μs. The height (measured from the centroid of patch elements) of Rx was fixed at 1.7 m from ground at all times, while the height of Tx was fixed at either 1.7 m for peer-to-peer measurements, or 2.4-3.0 m to emulate an access point. Dynamic measurements were conducted such that the Tx was fixed at a specific location, while the Rx was slowly pushed (≈0.2 m/s) along a convenient path with a customised measurement trolley. While the Rx was being pushed, 1 MIMO snapshot (16×16) was recorded every 15.36 ms. For more detailed descriptions of the measurement and environments, interested reader is referred to [8][9].

B. Multipath Parameters Extraction

For the development of stochastic physical channel models, the multipath parameters, such as the time delay of arrival (TDoA), DoD, DoA, and Doppler shift, must be extracted from the measurement raw data. In order to increase implementation efficiency with circular arrays and reduce overall processing time with vast database, we employed the 3-D Hybrid-Space Space-Alternating Generalised Expectation-maximisation (HS-SAGE) algorithm [10] to extract the TDoA, DoA, DoD, and path gain of the MPCs. The HS-SAGE algorithm extracted the multi-dimensional parameter in a combination of element-space and beamspace domains (and hence the notation 'hybrid-space'). In beamspace processing, a number of beams were formed across the subset of the entire supportable estimation space (certain conditions applied, see [10]). Iterative estimation processes were only executed across the 'hybrid-space' data of reduced dimensionality in terms of input data size, thus a reduction in overall computing resources and effective computation time.

For this particular exercise, both DoAs and DoDs were estimated in the normal element-space domain, while the TDoAs were estimated in the beamspace domain focusing in 0-400 ns temporal region as it was observed that (almost) all MPCs concentrated in this region within the 30 dB power window (from the strongest path). Each set of results was estimated from five consecutive MIMO snapshots along the dynamic path. With more than 15 Gbytes of compressed raw database, the extracted

3-D multipath parameter data can now be used to represent meaningful and realistic statistics as observed in a real MIMO radio environment.

C. Summary of Double-Directional 'General Trend' Results

The scope of this paper is focused on DoA (ϕ_{Rx}) and DoD (ϕ_{Tx}) azimuth domains, albeit the support of TDoA extraction from the 3-D HS-SAGE algorithm. Since the measurements were conducted in dynamic mode, the directional parameters associated to a particular MPC changed as a function of mobile Rx displacement along the dynamic route. In order to gain a better insight into the overall dependency between the directional parameters, the Tx and Rx circular array orientations were artificially readjusted offline such that both faced each other at their respective normalised 0° reference axis throughout the whole dynamic path. This directional normalisation procedure was performed manually by visual inspection, based on the knowledge of estimated multipath parameters[1], as well as the geometrical structure of the environments (to the best accuracy based on environment blueprints). Hence, the resultant results effectively represent instantaneous spatial distributions of the MPCs, for any realisation of the MIMO channel in environments of similar nature.

Fig. 1 presents a sample of the DoA-DoD joint distribution corresponding to measurement results in the open foyer environment (floor plan in [9]). As can be clearly seen in the figure, the joint distribution has a '*general trend*' showing that considerable amount of MPCs (>50%) tend to concentrate around the directional regions aligned to the axis where both terminals faced each other, as well as regions in which either one faced the opposite direction. Although not presented here, the same trend can also be seen in other joint distributions corresponding to measurements in other indoor environments (reported in [8] and [9]).

The so-called '*trend*' shows that most MPCs tend to concentrate around the directional regions where both Tx and Rx face each other, such that both DoAs and DoDs are not evenly and independently distributed around the azimuth. This again highlights the main motivation behind the work, that is to model the '*general trend*' of the DoA-DoD joint statistics with correlations taken into account.
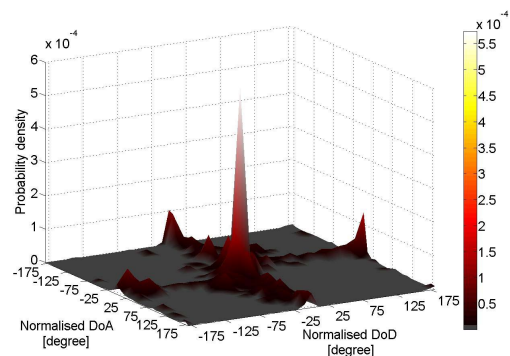

Figure 1: DoA and DoD joint distribution in the foyer environment (probability density is shading coded)

---

[1] It was observed that in most cases, including in a complete NLOS condition, the DoA of the strongest path was always facing the angular location of the Tx, and vice-versa for the DoD [8][9].

Note that the '*general trend*' phenomenon can only be clearly observed after the directional normalisation procedure described above. In summary, there are three 'Regions' where significant concentration of MPCs can be found:

- *Region A*: $\phi_{Tx} \in [-50°, 50°]$, $\phi_{Rx} \in [-50°, 50°]$,
- *Region B*: $\phi_{Tx} \in [-50°, 50°]$, $\phi_{Rx} \in [-180°, -130°] \cup [130°, 180°]$,
- *Region C*: $\phi_{Tx} \in [-180°, -130°] \cup [130°, 180°]$, $\phi_{Rx} \in [-50°, 50°]$.

Here, 0° (at both Tx and Rx) is the angular reference direction where both terminals faced each other. All the extracted DoAs and DoDs corresponding to all measurements are normalised to this reference. Also, the angular location of 180° is physically equivalent to -180°.

III. Modelling Approach Revisited[2]

Since majority MPCs concentrated in the '*general trend*' regions, the paper considers the modelling framework for the DoAs and DoDs within these three regions as commonly observed in the joint distributions of different picocell radio environments. The proposed framework provides alternative means to generate MIMO channel responses based on 'double-directional' approach, and is generic to all measured environments and propagation conditions.

In order to generate a complete MIMO model, additional features of the channel (e.g. clustering phenomena, dynamic evolutions of MPCs, TDoA distributions, etc.) can be included as an overlay of the framework, such that special propagation conditions (e.g. far scatterers, number of clusters) can be customised according to the specific behaviour of the environments. However, space limitation does not allow a comprehensive treatment of these additional features here. Interested reader is referred to the COST 273 modelling approaches [1] for detailed discussions on these additional items beyond the scope of this paper.

The modelling work begins by first identifying a suitable distribution for the angular domain. The most common angular distributions considered by researchers in this field are the normal, Laplacian (double exponential), and Von Mises distributions. Our analysis reveals that the directional parameter is close to Laplacian distributed (see [11] for the fitted results). In addition, the joint distributions of DoA and DoD in Regions A, B, and C also exhibit 'dual-Laplacian' (or bivariate exponential) characteristics when viewed from their respective domains. This phenomenon is observed visually from the joint distributions (e.g. Fig. 1).

Hence, the proposed model for the joint distributions should also exhibit Laplacian characteristics in the dual-spatial domain, which can be achieved using a *2-D Laplacian*-like approach, or more commonly known as the bivariate exponential approach. Several bivariate exponential distributions have been derived (presented in [12][13]), e.g. Arnold and Strauss', Hougaard's, Downton's, Gumbel's, Freund's, Marshall and Olkin's, etc. Under certain constraints such as the range of correlation coefficients (ρ) of the two random data, these bivariate

exponential functions can be fitted to the observed data. For example, the Farlie-Gumbel-Morgenstern distribution [13] requires that $|\rho| \leq 1/3$ in order for it to be used to fit the measured DoA and DoD data here. However, these functions involve a number of variables and sophisticated sub-expressions, which have directly increased the numerical complexity and computational burden of the model. Some expressions also involve complicated numerical routines that are most of the times difficult to accomplish while preserving accuracy.

It should be noted that the development of a model must be made simple with elegant formulation, and yet able to preserve as many important properties and characteristics of the channel as possible, and with minimum compensation in terms of accuracy and reliability. Knowing that it is challenging to realise all the criteria simultaneously, certain compromises between them must be made. In light of that, we propose a *modified Gumbel's bivariate exponential expression* to model the DoA-DoD joint distribution. The proposed approach adopts the original Gumbel's bivariate exponential function [12], since it is able to model the bivariate exponentially distributed 2-D data with certain correlation coefficient. The proposed expression common for different 'Region' is given by:

$$f(\phi_{Tx}^{(i)}, \phi_{Rx}^{(i)}) \propto \exp\left(\begin{array}{c} -\left|\dfrac{\phi_{Tx}^{(i)} - \mu_{Tx}^{(i)}}{\sigma_{Tx}^{(i)}/\sqrt{2}}\right| - \left|\dfrac{\phi_{Rx}^{(i)} - \mu_{Rx}^{(i)}}{\sigma_{Rx}^{(i)}/\sqrt{2}}\right| - \\ \gamma_i \left|\dfrac{\phi_{Tx}^{(i)} - \mu_{Tx}^{(i)}}{\sigma_{Tx}^{(i)}/\sqrt{2}}\right| \left|\dfrac{\phi_{Rx}^{(i)} - \mu_{Rx}^{(i)}}{\sigma_{Rx}^{(i)}/\sqrt{2}}\right| \end{array} \right) \quad (1),$$

such that $\phi_{Tx}^{(i)} \sim \text{Laplace}(\mu_{Tx}^{(i)}, \sigma_{Tx}^{(i)}/\sqrt{2})$ (2),

$$f(\phi_{Tx}^{(i)}) = \frac{\sqrt{2}}{\sigma_{Tx}^{(i)}} \exp\left(\left|\frac{\phi_{Tx}^{(i)} - \mu_{Tx}^{(i)}}{\sigma_{Tx}^{(i)}/\sqrt{2}}\right| \right) \quad (3),$$

and $\phi_{Rx}^{(i)} \sim \text{Laplace}(\mu_{Rx}^{(i)}, \sigma_{Rx}^{(i)}/\sqrt{2})$ (4),

$$f(\phi_{Rx}^{(i)}) = \frac{\sqrt{2}}{\sigma_{Rx}^{(i)}} \exp\left(\left|\frac{\phi_{Rx}^{(i)} - \mu_{Rx}^{(i)}}{\sigma_{Rx}^{(i)}/\sqrt{2}}\right| \right) \quad (5),$$

where the notational superscript '*i*' in parenthesis denotes a specific 'Region' ($i \in \{A, B, C\}$), $(\sigma_{Tx}^{(i)}, \sigma_{Rx}^{(i)})$ denotes the DoD/DoA standard deviation in 'Region-*i*', $(\mu_{Tx}^{(i)}, \mu_{Rx}^{(i)})$ is the mean of DoD/DoA in 'Region-*i*', and $\gamma_i \in [0,1]$ is related to the correlation coefficient in 'Region-*i*', ρ_i. For the case of a Gumbel's bivariate exponential distribution [12], the relationship of γ_i and ρ_i, is given as

$$\rho_i = -1 - \frac{1}{\gamma_i} \exp(1/\gamma_i) E(-1/\gamma_i) \quad (6),$$

and $E(\cdot)$ is the exponential integral function defined by:

$$E(x) = -\int_{-x}^{\infty} \frac{\exp(-y)}{y} dy \quad (7).$$

The above expressions are applied separately in different 'Regions', with different sets of $\sigma_{Tx}^{(i)}$, $\sigma_{Rx}^{(i)}$, $\mu_{Tx}^{(i)}$, $\mu_{Rx}^{(i)}$, and γ_i, where $i \in \{A, B, C\}$. When generating the pair wise random DoA and DoD data using the proposed expression in (1), the ratio of the number of 2-D variates in Regions A, B, C, and the 'unaccounted Region (say *j*)' is given by $K_A: K_B: K_C: K_j$ (ratio summation equals 1). The ratio determines the probability of

---

[2] The authors' initial modelling work presented in [11] has been refined here in this section in order to improve accuracy.

the 2-D random variates (i.e. MPCs) falling into a specific 'Region'. Note that the sum of these ratios effectively represents the total number of MPCs in the channel, with K_A, K_B, and K_C reflecting the distribution of number of MPCs in the '*general trend*' Regions. (Recall that additional features must be added in the final model to represent a complete channel response, where these features effectively include other 'irregular' MPCs unaccounted here.) The final DoA-DoD joint distribution density for the complete channel response should also fulfill the following criterion:

$$\int_{\text{all}\phi_{\text{Rx}}^{(i)}} \int_{\text{all}\phi_{\text{Tx}}^{(i)}} f\left(\phi_{\text{Tx}}^{(i)},\phi_{\text{Rx}}^{(i)}\right) d\phi_{\text{Tx}}^{(i)} d\phi_{\text{Rx}}^{(i)} = 1-\varepsilon \; , \; \varepsilon < 0.5 \qquad (8),$$
$$i\in\{A,B,C\}$$

where ε represents the total density for other DoA and DoD components (i.e. irregular MPCs) that are beyond Regions A, B, and C, given by:

$$\varepsilon = \int_{\text{all}\phi_{\text{Rx}}^{(j)}} \int_{\text{all}\phi_{\text{Tx}}^{(j)}} f\left(\phi_{\text{Tx}}^{(j)},\phi_{\text{Rx}}^{(j)}\right) d\phi_{\text{Tx}}^{(j)} d\phi_{\text{Rx}}^{(j)} \qquad (9).$$
$$j\notin\{A,B,C\}$$

Here, $\varepsilon < 0.5$ since majority of the MPCs are found to be concentrated in the '*general trend*' Regions. However, since the work focuses on the double-directional '*general trend*' modelling, the additional features contributing to the density in ε is beyond the scope of discussion here.

IV. 2-D RANDOM NUMBER GENERATION

In order to further reduce the complexity, the random number generation process across the DoA and DoD domains can be implemented separately in 1-D case as follows. We assume the joint distribution of DoA and DoD can be independently factored into ϕ_{Tx} and ϕ_{Rx} and can be written as

$$f\left(\phi_{\text{Tx}}^{(i)},\phi_{\text{Rx}}^{(i)}\right) \propto \exp\left(-\left|\frac{\phi_{\text{Tx}}^{(i)} - \mu_{\text{Tx}}^{(i)}}{\sigma_{\text{Tx}}^{(i)}/\sqrt{2}}\right|\right) \exp\left(-\left|\frac{\phi_{\text{Rx}}^{(i)} - \mu_{\text{Rx}}^{(i)}}{\sigma_{\text{Rx}}^{(i)}/\sqrt{2}}\right|\right) \qquad (10).$$

Take note that the above expression only holds true when both DoA and DoD are both uncorrelated, or is statistically proven to be uncorrelated ($\rho \approx 0$ then $\gamma \approx 0$).

On the other hand, if the correlation of DoA and DoD is significant, the 2-D random numbers (of bivariate exponential or Laplace distributed) must be generated taking their correlations into account. Owing to the complexities of generating joint Laplace variates (ϕ_{Tx}, ϕ_{Rx}) directly with a correlation coefficient ρ (see [14] where the authors applied sophisticated moment-based and maximum-likelihood approaches), here we propose an elegant transformation technique to generate the variates of each pair ϕ_{Tx} and ϕ_{Rx}. For simplicity, the superscript notation '*i*' used above to denote Region A, B, or C is excluded from the following variables, since the same approach can be applied in all three Regions. Note that the proposed transformation technique in the following complies with the modelling criteria stated above, i.e. simplicity and preservation of correlation information of the variates for improved accuracy.

Assuming $\phi_{\text{Tx}} \sim \text{Laplace}(\mu_{\text{Tx}},\beta_{\text{Tx}})$, $\phi_{\text{Rx}} \sim \text{Laplace}(\mu_{\text{Rx}},\beta_{\text{Rx}})$, where $\beta_{\text{Tx}} = \sigma_{\text{Tx}}/\sqrt{2} > 0$, $\beta_{\text{Rx}} = \sigma_{\text{Rx}}/\sqrt{2} > 0$, and the correlation coefficient of ϕ_{Tx} and ϕ_{Rx} is ρ. Hence we can also write

$$\widetilde{\phi}_{\text{Tx}} = \phi_{\text{Tx}} - \mu_{\text{Tx}} \sim \text{Laplace}(0, \beta_{\text{Tx}}) \qquad (11),$$

$$\widetilde{\phi}_{\text{Rx}} = \phi_{\text{Rx}} - \mu_{\text{Rx}} \sim \text{Laplace}(0, \beta_{\text{Rx}}) \qquad (12).$$

Furthermore by taking the absolute values of the above Laplace variates we have

$$W_{\text{Tx}} = \left|\widetilde{\phi}_{\text{Tx}}\right| \sim \exp(1/\beta_{\text{Tx}}) \qquad (13),$$

$$W_{\text{Rx}} = \left|\widetilde{\phi}_{\text{Rx}}\right| \sim \exp(1/\beta_{\text{Rx}}) \qquad (14),$$

and from Jensen's inequality and also from Cauchy-Schwarz relationship [15]:

$$\left|\text{E}\left(\widetilde{\phi}_{\text{Tx}}\widetilde{\phi}_{\text{Rx}}\right)\right| \leq \text{E}\left(\left|\widetilde{\phi}_{\text{Tx}}\right|\left|\widetilde{\phi}_{\text{Rx}}\right|\right) \leq \sqrt{\text{E}\left(\left|\widetilde{\phi}_{\text{Tx}}\right|^2\right)\text{E}\left(\left|\widetilde{\phi}_{\text{Rx}}\right|^2\right)} \qquad (15),$$

we can therefore deduce that the correlation coefficient of W_{Tx} and W_{Rx} is $\delta = |\rho|$ where $\delta \in [0,1]$.

In order to form W_{Tx} and W_{Rx} we can let $X_{\text{Tx}} \sim \text{N}(0, \beta_{\text{Tx}})$, $Y_{\text{Tx}} \sim \text{N}(0, \beta_{\text{Tx}})$, so that X_{Tx} and Y_{Tx} are both independent, and $\text{Var}(X_{\text{Tx}}) = \text{Var}(Y_{\text{Tx}}) = \beta_{\text{Tx}}$.

In addition we also let

$$X_{\text{Rx}} = \sqrt{\frac{\delta\beta_{\text{Rx}}}{\beta_{\text{Tx}}}}X_{\text{Tx}} + \sqrt{1-\delta}\,G \qquad (16),$$

$$Y_{\text{Rx}} = \sqrt{\frac{\delta\beta_{\text{Rx}}}{\beta_{\text{Tx}}}}Y_{\text{Tx}} + \sqrt{1-\delta}\,H \qquad (17),$$

such that $G, H \sim \text{N}(0, \beta_{\text{Rx}})$ and both G and H are independent normal variables. Hence we can easily show that $X_{\text{Rx}} \sim \text{N}(0, \beta_{\text{Rx}})$, $Y_{\text{Rx}} \sim \text{N}(0, \beta_{\text{Rx}})$, X_{Rx} and Y_{Rx} are both independent and $\text{Var}(X_{\text{Rx}}) = \text{Var}(Y_{\text{Rx}}) = \beta_{\text{Rx}}$.

In order to form W_{Tx} and W_{Rx} we can set

$$W_{\text{Tx}} = 0.5(X_{\text{Tx}}^2 + Y_{\text{Tx}}^2) \sim \exp(1/\beta_{\text{Tx}}) \qquad (18),$$

$$W_{\text{Rx}} = 0.5(X_{\text{Rx}}^2 + Y_{\text{Rx}}^2) \sim \exp(1/\beta_{\text{Rx}}) \qquad (19),$$

and it can be easily verified that the coefficient correlation between W_{Tx} and W_{Rx} is δ.

In order to form the Laplace variates $\widetilde{\phi}_{\text{Tx}}$ and $\widetilde{\phi}_{\text{Rx}}$, we can follow the above steps to find two sets of independent variates such that

$$W_{\text{Tx}}^{(1)}, W_{\text{Tx}}^{(2)} \sim \exp(1/\beta_{\text{Tx}}) \qquad (20),$$

$$W_{\text{Rx}}^{(1)}, W_{\text{Rx}}^{(2)} \sim \exp(1/\beta_{\text{Rx}}) \qquad (21),$$

where $W_{\text{Tx}}^{(1)}$ is independent of $W_{\text{Tx}}^{(2)}$ and $W_{\text{Rx}}^{(1)}$ is independent of $W_{\text{Rx}}^{(2)}$, and the superscript argument in parenthesis denotes the sequence of the generated variates.

Hence, to form back the Laplace variates we can set

$$\widetilde{\phi}_{\text{Tx}} = W_{\text{Tx}}^{(1)} - W_{\text{Tx}}^{(2)} \sim \text{Laplace}(0, \beta_{\text{Tx}}) \qquad (22),$$

$$\widetilde{\phi}_{\text{Rx}} = W_{\text{Rx}}^{(1)} - W_{\text{Rx}}^{(2)} \sim \text{Laplace}(0, \beta_{\text{Rx}}) \qquad (23).$$

In the event that the sign of the correlation coefficient of $\widetilde{\phi}_{\text{Tx}}$ and $\widetilde{\phi}_{\text{Rx}}$ is directly opposite of ρ we can form $\widetilde{\phi}_{\text{Tx}}$ and $\widetilde{\phi}_{\text{Rx}}$ by setting $\widetilde{\phi}_{\text{Tx}} \leftarrow -\widetilde{\phi}_{\text{Tx}}$ or $\widetilde{\phi}_{\text{Rx}} \leftarrow -\widetilde{\phi}_{\text{Rx}}$.

Finally, by setting $\widetilde{\phi}_{\text{Tx}} + \mu_{\text{Tx}}$, $\widetilde{\phi}_{\text{Rx}} + \mu_{\text{Rx}}$ we recover back

$$\phi_{\text{Tx}} = \widetilde{\phi}_{\text{Tx}} + \mu_{\text{Tx}} \sim \text{Laplace}(\mu_{\text{Tx}}, \beta_{\text{Tx}}) \qquad (26),$$

$$\phi_{\text{Rx}} = \widetilde{\phi}_{\text{Rx}} + \mu_{\text{Rx}} \sim \text{Laplace}(\mu_{\text{Rx}}, \beta_{\text{Rx}}) \qquad (27),$$

where the coefficient correlation of ϕ_{Tx} and ϕ_{Rx} is ρ.

V. Modelling Results in Real Environments

The '*general trend*' of the MIMO channel is modelled using the proposed methods with parameters obtained from real measurement environments. The calculated $|\rho_i|$ and K_i values in different indoor environments are presented in Table 1 (computed using vast database of extracted DoAs and DoDs, >50,000 sets in most cases), for measurements corresponding to Tx height at 1.7 m. It can be seen that ρ_i has a low value in most cases, and can be modeled using expression in (10) (especially for Office LOS since $|\rho_i| \to 0$). However, the correlation coefficients for 'Office (OLOS/NLOS) Regions B and C' and 'Open Foyer' are significantly higher, such that the pair wise DoA and DoD variates must be modelled with their correlations taken into considerations. Further, from the calculated values of K_i (number of MPCs in 'Region i'), the hypothesis of most MPCs tend to concentrate in Regions A, B, and C is validated. From the percentage of power distributions, it can also be seen to a great extent that most of the stronger MPCs concentrate only in Region A in all cases, which corresponds to the directional region where both Tx and Rx face each other.

Environment	Region	$|\rho_i|$	K_i	Power %
Office (LOS)	A	0.0209	0.4686	82.38
	B	0.0147	0.1188	1.67
	C	0.0594	0.1869	11.51
Office (OLOS/ NLOS)	A	0.0891	0.2770	60.20
	B	0.6005	0.1081	5.12
	C	0.5460	0.1309	6.61
Open Foyer (LOS/OLOS)	A	0.1810	0.3094	67.40
	B	0.5974	0.1087	3.58
	C	0.5319	0.1478	15.60
Corridor (LOS)	A	0.0184	0.4552	87.93
	B	0.1006	0.1559	3.56
	C	0.2592	0.1236	3.21

Table 1: Calculated values of $|\rho_i|$, K_i and percentage power, $i \in \{A, B, C\}$

We have presented the joint distribution of DoA and DoD in Regions A, B, and C of an office environment (LOS) in [11]. For that particular example, the 2-D DoA and DoD variates for all three Regions are generated using the simplified function given in (10), since $\rho = O(10^{-2})$ and $\gamma \approx 0$. Here, since the correlation coefficients of DoAs and DoDs in the foyer environment are significantly higher, the joint distribution in all three Regions is modelled using the proposed *modified Gumbel's bivariate exponential expression* given in (1), where the pair wise DoA and DoD variates are generated using the proposed transformation technique described in Section IV. Fig. 2 presents the joint distribution (total volume normalised to 1) of the simulated DoA and DoD variates for the open foyer environment, and its calculated parameters from measurement data are tabulated in Table 2. The new parameter values computed from the simulated data are given in parenthesis in Table 2, where it can be seen that they match closely with the calculated values from measurements. From the '*general trend*' results extracted from real measurement data in Fig. 3, it can again be appreciated that the agreement between both simulated and measured data is remarkable using the proposed approaches.
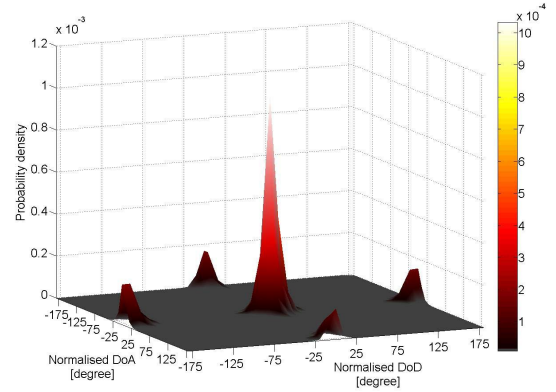

Figure 2: Joint density plot for the simulated DoA and DoD '*general trend*' data in the foyer environment
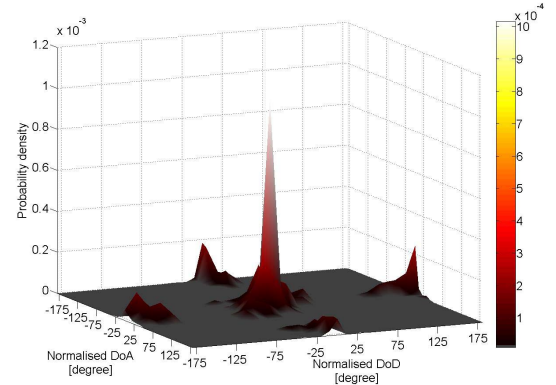

Figure 3: Joint density plot for the DoA and DoD '*general trend*' data in the foyer environment obtained from measurement results

Region	$f\left(\phi_{Tx}^{(i)}, \phi_{Rx}^{(i)}\right)$, units in degrees				$|\rho_i|$
	$\mu_{Tx}^{(i)}$	$\sigma_{Tx}^{(i)}$	$\mu_{Rx}^{(i)}$	$\sigma_{Rx}^{(i)}$	
A	-1.19 (-1.17)	10.05 (10.16)	-0.87 (-0.84)	10.32 (10.83)	0.1810 (0.1774)
B	-2.34 (-2.35)	7.24 (7.60)	0.35 (0.52)	12.70 (14.87)	0.5974 (0.4932)
C	1.58 (1.51)	9.93 (14.96)	2.40 (2.39)	9.93 (11.00)	0.5319 (0.3511)

Table 2: Parameters of the modified Gumbel's bivariate exponential functions for the foyer environment, $i \in \{A, B, C\}$
(values in parenthesis are computed from the simulated data)

In addition, it was found that the power azimuth spectrum (PAS) at both the Tx and Rx also exhibited Laplacian-like characteristics [8][9], where majority of the strong components are concentrated in 'Region A' (see power distributions in Table 1). Hence, the same bivariate approach can be applied to model the joint power density. Similarly, in the case of weak association between both DoA and DoD, the expression for the joint power density can be simplified to:

$$P\left(\phi_{Tx}^{(i)}, \phi_{Rx}^{(i)}\right) \propto \exp\left(-\left|\frac{\phi_{Tx}^{(i)} - \hat{\mu}_{Tx}^{(i)}}{\hat{\sigma}_{Tx}^{(i)} / \sqrt{2}}\right|\right) \exp\left(-\left|\frac{\phi_{Rx}^{(i)} - \hat{\mu}_{Rx}^{(i)}}{\hat{\sigma}_{Rx}^{(i)} / \sqrt{2}}\right|\right) \quad (28),$$

where $\hat{\mu}_{Tx}$ and $\hat{\mu}_{Rx}$ are respectively the 1st moment of the PAS at Tx and Rx, and $\hat{\sigma}_{Tx}$ and $\hat{\sigma}_{Rx}$ are the square root of 2nd central moment of the PAS at Tx and Rx, respectively. In the case of significant correlations, the joint power density function can be represented by:

$$P\left(\phi_{Tx}^{(i)}, \phi_{Rx}^{(i)}\right) \propto \exp\left(-\left|\frac{\phi_{Tx}^{(i)} - \hat{\mu}_{Tx}^{(i)}}{\hat{\sigma}_{Tx}^{(i)} / \sqrt{2}}\right| - \left|\frac{\phi_{Rx}^{(i)} - \hat{\mu}_{Rx}^{(i)}}{\hat{\sigma}_{Rx}^{(i)} / \sqrt{2}}\right| - \gamma_i \left|\frac{\phi_{Tx}^{(i)} - \hat{\mu}_{Tx}^{(i)}}{\hat{\sigma}_{Tx}^{(i)} / \sqrt{2}}\right| \left|\frac{\phi_{Rx}^{(i)} - \hat{\mu}_{Rx}^{(i)}}{\hat{\sigma}_{Rx}^{(i)} / \sqrt{2}}\right|\right) \quad (29).$$

Using the expression in (29), the simulated joint power density in 'Region A' of the foyer environment is presented in Fig. 4, where the result also matches well with that from the measurements shown in Fig. 5. In this particular example, the parameters in (29) are determined using spatial statistics approach [16] (a statistical technique for multi-dimensional fitting), with values: $(\hat{\sigma}_{Tx}, \hat{\sigma}_{Rx}) = (9.0°, 11.7°)$, and $(\hat{\mu}_{Tx}, \hat{\mu}_{Rx}) = (0°, 0°)$. From Kolmogorov-Smirnov goodness of fit test (D = 0.3679) [16], it is found that at 5% significance level, the error is $P_{err}^{(i)} \sim NID(0, 0.0258)$, where $P_{err}^{(i)} = P_{measured}^{(i)} - P_{simulated}^{(i)}$, $i \in 1, 2, \ldots, N$, and N is the sample size (N = 30,000 in this example). With such an error distribution, it can be assured that the proposed expression in (29) can facilitate realistic and meaningful statistical representation of the joint power density.
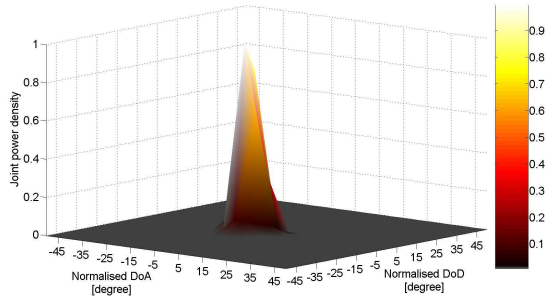

Figure 4: Joint power density plot at 'Region A' in the foyer environment using spatial statistics (peak normalised to 1)
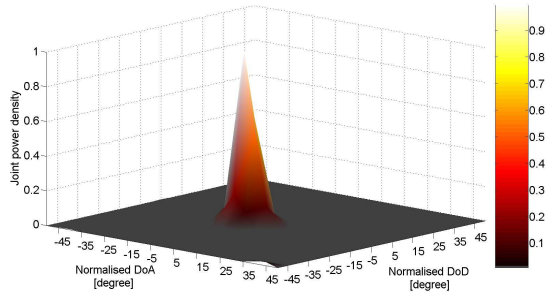

Figure 5: Joint power density plot at 'Region A' in the foyer environment using the measurement results (peak normalised to 1)

VI. CONCLUDING REMARKS

This paper has presented a new modelling approach for the joint distributions of the double-directional components, as well as their joint power density. In order to take the characterised correlation coefficients into account, the paper proposes a *modified Gumbel's bivariate exponential expression* to model the '*general trend*' of the double-directional components as observed from the indoor measurement experiments, where the pair wise DoA and DoD components (of certain correlation) are generated using the proposed transformation technique. It is shown that results from the proposed approaches match well with that from the real measurement data, hence the accuracy

of the statistical properties of the simulated data is successfully preserved. More importantly, the proposed approaches comply with the fundamental criteria in stochastic modelling, where the simulation procedure should ideally be non-complicated with minimum sacrifice in accuracy and reliability.

It should be noted that the main focus of this paper is to model the common '*trend*' (i.e. Regions A, B and C as indicated in paper) as observed in the measured indoor environments. The approach is generic, and can form an overlay framework in other stochastic MIMO models (e.g. COST 273 [1] and IST WINNER [2]) in terms of generation of double-directional random components. Additional modelling procedures (e.g. clustering, delays, multipath dynamics as birth-death statistics [17], etc.) must still be included in the final model in order to generate complete MIMO responses specific to various unique characteristics in different environments.

REFERENCES

[1] L. M. Correia, 'Mobile broadband multimedia networks – Techniques, models and tools for 4G,' Academic Press, 2006, ISBN 0123694221.

[2] J. Meinilä et al., 'A set of channel and propagation models for early link and system level simulations,' IST WINNER D5.1 report, IST-2003-507581.

[3] Network of Excellence in Wireless Communications (NEWCOM), http://newcom.ismb.it/public/index.jsp, dated 28 August 2006.

[4] 802.11 TGn Channel Models, IEEE 802.11-03/940r4, May 2004.

[5] L. Schumacher, J. P. Kermoal, F. Frederiksen, K. I. Pedersen, A. Algans, and P. E. Mogensen, 'MIMO channel characterisation,' D2 ver. 1.1, IST-1999-11729 METRA, February 2001.

[6] H. Özcelik et al., 'Deficiencies of the Kronecker MIMO radio channel model,' COST 273 TD(03)123, Paris, France, 20-23 May 2003.

[7] L. Schumacher, K.I. Pedersen, and P.E. Mogensen, 'From antenna spacings to theoretical capacities – Guidelines for simulating MIMO systems,' 13th IEEE PIMRC, Lisbon, Portugal, 15-18 September 2002.

[8] C. M. Tan, M. A. Beach, and A. R. Nix, 'Statistical characterisation of double-directional channels in modern office environments,' 2nd SPWC, London, UK, 2-4 June 2004.

[9] C. M. Tan, D. L. Paul, M. A. Beach, A. R. Nix, and C. J. Railton, 'Dynamic double-directional propagation channel analysis with dual circular arrays,' COST 273/284 Workshop, Sweden, 7-10 June 2004.

[10] C. M. Tan, M. A. Beach, and A. R. Nix, 'Multidimensional hybrid-space SAGE algorithm: Joint element-space and beamspace processing,' IST Mobile and Wireless Communications Summit 2003, Aveiro, Portugal, 15-18 June 2003.

[11] C. M. Tan, C. M. Chin, M. L. Sim, and M. A. Beach, 'Modelling the general dependency between directions of arrival and departure for an indoor MIMO channel,' 63rd IEEE VTC, Melbourne, 7-10 May 2006.

[12] S. Nadarajah, and S. Kotz, 'Reliability for some bivariate exponential distributions,' Technical report, University of Nebraska, USA.

[13] I. Bairamov, S. Kotz, and M. Bekçi, 'New generalised Farlie-Gumbel-Morgenstern distributions and concomitants of order statistics,' Technical report, Ankara University, Turkey.

[14] T. Eltoft, T. Kim, and T. W. Lee, 'On the multivariate Laplace distribution,' IEEE Sig. Proc. Letters, vol. 13, May 2006, pp. 300-303.

[15] S. F. Arnold, 'Mathematical statistics,' Prentice-Hall, USA, 1990.

[16] W. N. Venables, and B. D. Ripley, 'Modern applied statistics with S,' 4th Edition, Springer, 2002.

[17] C. C. Chong, C. M. Tan, D. I. Laurenson, S. McLaughlin, M. A. Beach, and A. R. Nix, 'A novel wideband dynamic directional indoor channel model based on a Markov process,' IEEE Transactions on Wireless Communications, vol. 4, no. 4, July 2005, pp. 1539-1552.